

Influence on photonic crystal fiber dispersion of the size of air holes in different rings within the cladding

Yanfeng Li (栗岩锋), Bowen Liu (刘博文), Zihan Wang (王子涵),
Minglie Hu (胡明列), and Qingyue Wang (王清月)

Ultrafast Laser Laboratory, College of Precision Instrument and Optoelectronics Engineering, Tianjin University;
Key Laboratory of Optoelectronics Information and Technical Science (Tianjin University),
Ministry of Education, Tianjin 300072

Received November 20, 2003

The influence on photonic crystal fiber dispersion of the size of air holes in different rings within the cladding is investigated using a semivectorial finite difference method. Numerical results reveal that the photonic crystal fiber dispersion is more sensitive to the variation of the air hole size in the first and second rings, indicating that design of photonic crystal fibers with desirable dispersion properties requires more precise control of the parameters of the air holes in the vicinity of the fiber core.

OCIS codes: 060.2310, 060.2270, 060.2400.

Photonic crystal fibers (PCFs)^[1], also known as microstructured optical fibers or holey fibers, whose cladding is composed of a two-dimensional (often periodic) array of closely packed glass capillaries drawn at a high temperature, have attracted much attention in the last few years. PCFs guide light by modified total internal reflection or photonic bandgap effect, depending on the particular fiber design^[2], and therefore the fibers are referred to as index-guiding PCFs or photonic bandgap fibers, respectively.

The wavelength-dependent cladding index of the index-guiding PCFs has led to a number of interesting properties such as the endless single-mode behavior^[3] and widely tunable dispersion^[4–9]. PCFs can have anomalous dispersion in the visible part of the spectrum^[4] and thus have greatly enriched the nonlinear phenomena that can be achieved with these fibers^[10,11]. PCFs can also display large normal dispersion in the long wavelength part and can be designed as dispersion-compensating fibers^[5,6]. Finally, flattened dispersion can be achieved with a proper choice of the fiber parameters^[7–9].

Complex fiber structures have been proposed where the air holes in different rings within the PCF cladding can have different sizes so as to obtain flattened dispersion^[8,9]. A schematic of such a design is shown in Fig. 1, where the second ring of air holes have a larger size than the other air holes. However, the influence on PCF dispersion of the air hole size of an individual ring has not been investigated. In this letter, we have studied the influence on photonic crystal fiber dispersion of the size of air holes in different rings within the cladding using a semivectorial finite difference method. Numerical results show that for a particular fiber a 10% variation of the air hole size in the first and second rings results in a shift of the zero-dispersion-wavelength (ZDW) by 20 and 5 nm respectively and that the dispersion is not affected much by the air hole size variation in the third ring and the rings farther from the fiber core. The sensitivity of PCF dispersion to air hole size variation in the first two rings indicates that precise control of the parameters of the air holes in the vicinity of the fiber core is needed in designing PCFs with desirable dispersion properties.

In the semivectorial finite difference method^[12], we start with the two decoupled wave equations

$$\frac{\partial^2 E_x}{\partial x^2} + \frac{\partial}{\partial x} \left(\frac{1}{\varepsilon_r} \frac{\partial \varepsilon_r}{\partial x} E_x \right) + \frac{\partial^2 E_x}{\partial y^2} + (k_0^2 \varepsilon_r - \beta^2) E_x = 0, \quad (1)$$

$$\frac{\partial^2 E_y}{\partial y^2} + \frac{\partial}{\partial y} \left(\frac{1}{\varepsilon_r} \frac{\partial \varepsilon_r}{\partial y} E_y \right) + \frac{\partial^2 E_y}{\partial x^2} + (k_0^2 \varepsilon_r - \beta^2) E_y = 0. \quad (2)$$

where E_x and E_y are the two orthogonal components of the transverse electric field, ε_r is the relative permittivity, k_0 is the wave number in vacuum, and $\beta = k_0 n_{\text{eff}}$ is the propagation constant with n_{eff} being the modal effective index.

Using a five-point difference scheme, a difference equation can be obtained for E_x and E_y ^[13]

$$\alpha_w E_{p-1,q} + \alpha_e E_{p+1,q} + \alpha_n E_{p,q-1} + \alpha_s E_{p,q+1} + (\alpha_x + \alpha_y) E_{p,q} + \{k_0^2 \varepsilon_r(p,q) - \beta^2\} E_{p,q} = 0. \quad (3)$$

For E_x , the coefficients are $\alpha_w = \frac{2}{h^2} \frac{\varepsilon_r(p-1,q)}{\varepsilon_r(p,q) + \varepsilon_r(p-1,q)}$, $\alpha_e = \frac{2}{h^2} \frac{\varepsilon_r(p+1,q)}{\varepsilon_r(p,q) + \varepsilon_r(p+1,q)}$, $\alpha_n = \frac{1}{h^2}$, $\alpha_s = \frac{1}{h^2}$, $\alpha_x = -\frac{4}{h^2} + \alpha_e + \alpha_w$, $\alpha_y = -\alpha_n - \alpha_s$, where p and q are node indices. For E_y , we have similar coefficients^[12].

Equation (3) can be written as an algebraic eigenvalue equation

$$[A] \{E\} = \beta^2 \{E\} = k_0^2 n_{\text{eff}}^2 \{E\}. \quad (4)$$

where $[A]$ is the coefficient matrix.

Solving Eq. (4) yields the modal effective index n_{eff} with its corresponding field distribution.

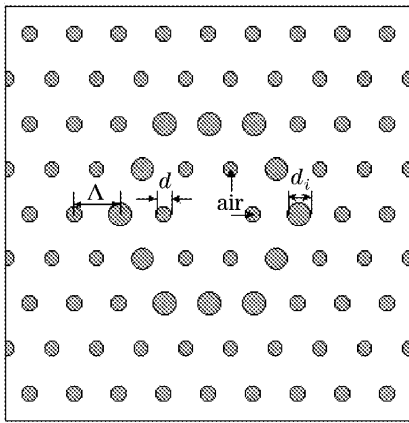


Fig. 1. Schematic of a PCF and its parameters.

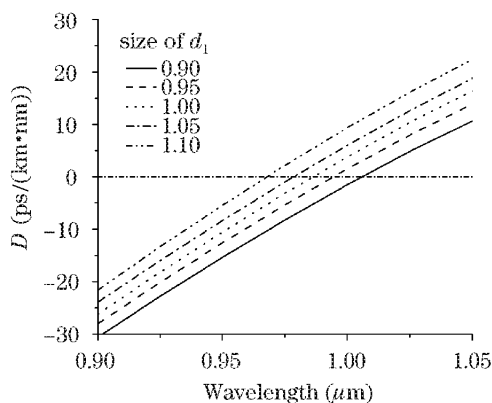


Fig. 2. Influence on PCF dispersion of the air hole size (in microns) in the first ring.

The structure of the air-silica PCF studied is illustrated in Fig. 1, where Λ is the fixed hole-to-hole spacing or pitch, d is the diameter of the regular air holes, and d_i is the diameter of the air holes in a certain ring that has been varied. The fiber parameters are chosen to be $\Lambda = 2.3 \mu\text{m}$ and $d = 1.0 \mu\text{m}$.

Figures 2 and 3 show how the air hole size variation in the first and second rings influences the ZDW, respectively, where material dispersion has been accounted for by the Sellmeier formula for silica. As is to be expected,

the influence of the air hole size variation in an individual ring on the PCF dispersion is the same as that of the variation of the size of all air holes simultaneously. Larger air holes in an individual ring will reduce the effective index of the cladding and increase the waveguide contribution to total dispersion^[7,9], thus shifting the ZDW to the shorter side of the spectrum, and vice versa, as shown in Figs. 2 and 3.

As a larger portion of the electric field is distributed within the first ring of air holes, the influence of the air hole size variation in the first ring is obviously stronger than that in the second ring. A 5% variation of the air hole size in the first ring results in a shift of the ZDW by about 8 nm and a 10% variation causes a larger shift of about 20 nm. A 5% and 10% variation of the air hole size in the second ring results in a shift of the ZDW by about 3 and 5 nm respectively, although the influence is not symmetric as in Fig. 2 when the air size becomes larger or smaller. We attribute this asymmetry to the smaller overlap between light field and air in the second ring. When the air hole size is comparable with the wavelength, increasing the air hole size in the second ring does not help to confine the light more appreciably while reducing it causes more light to escape into the air holes. This is consistent with the findings that an optimum air-filling ratio exists which minimizes the effective mode area and that reducing the air-hole size below

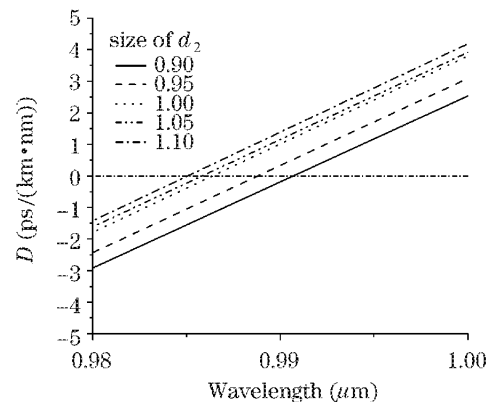


Fig. 3. Influence on PCF dispersion of the air hole size (in microns) in the second ring.

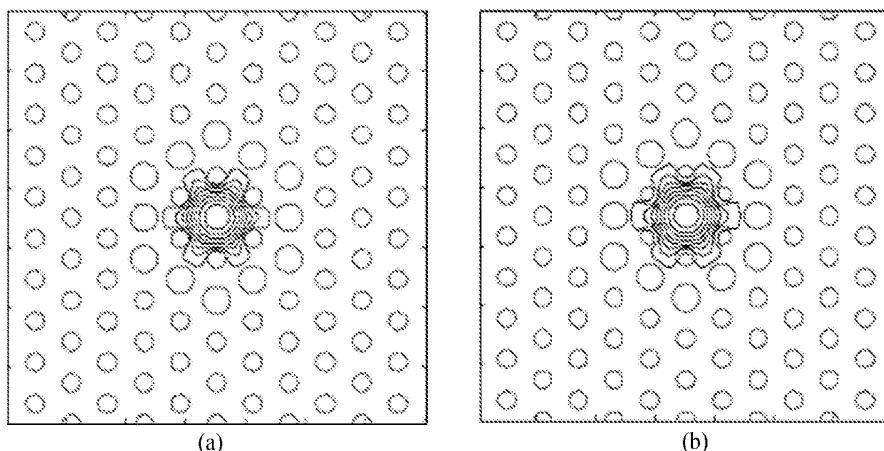


Fig. 4. Field distribution when the air holes in the second ring are larger than those in the other rings for (a) $\lambda = 800 \text{ nm}$ and (b) $\lambda = 1500 \text{ nm}$.

the optimum value influences the effective mode area more significantly than increasing the air-hole size above the optimum ratio (see the inset of Fig. 3 in Ref. [14]). In the longer wavelength side, the dispersion at 1550 nm is calculated to vary by about 10 and 2 ps/(nm·km) respectively when the air hole size in the first ring and second ring is changed by 10%. In agreement with the results in Ref. [9], the influence of the third ring and the rings farther from the core is negligible and not shown, because the electric field is mainly confined within the first two rings of the air holes around the fiber core, as is demonstrated in Fig. 4. It is important to note that enough rings of air holes are still required to reduce the confinement loss though their influence on dispersion is not so obvious^[9].

Understanding of the influence on PCF dispersion of air hole size in different rings has important implications. The shift of ZDW when the air size in a certain ring is slightly varied may result in different nonlinear phenomena as femtosecond laser pulses are propagated in PCFs. The sensitivity of PCF dispersion to air hole size variation in the first two rings implies that precise control of the size of air holes in the first two rings is needed in designing PCFs with flattened dispersion where dispersion variation should be no more than $1 - 2$ ps/(nm·km)^[7,8]. It may also explain the discrepancy between experimental and theoretical results in Ref. [15] in the context of flattened dispersion.

In conclusion, we have studied how the photonic crystal fiber dispersion is affected by the air hole size in different rings within the cladding. It is shown that the zero-dispersion-wavelength and the dispersion in the longer wavelength part are both sensitive to the air hole size variation in the first two rings, implying that precise control of the air hole parameters in the vicinity of the fiber core is required in designing photonic crystal fibers with desirable dispersion properties.

This work was supported by the National Natural Science Foundation of China (No. 60278003), the National Key Basic Research Special Foundation (NKBRSF) of

China (No. G1999075201 and 2003CB314904), and the National High Technology Programme of China (No. 2003AA311010). Y. Li's e-mail address is li-yanfeng@163.com.

References

1. J. C. Knight, T. A. Birks, P. St. J. Russell, and D. M. Atkin, *Opt. Lett.* **21**, 1547 (1996).
2. P. Russell, *Science* **299**, 358 (2003).
3. T. A. Birks, J. C. Knight, and P. St. J. Russell, *Opt. Lett.* **22**, 961 (1997).
4. J. C. Knight, J. Arriaga, T. A. Birks, A. Ortigosa-Blanch, W. J. Wadsworth, and P. St. J. Russell, *IEEE Photon. Technol. Lett.* **12**, 807 (2000).
5. T. A. Birks, D. Mogilevtsev, J. C. Knight, and P. St. J. Russell, *IEEE Photon. Technol. Lett.* **11**, 674 (1999).
6. Y. Ni, L. Zhang, and J. Peng, *Chin. Opt. Lett.* **1**, 385 (2003).
7. A. Ferrando, E. Silvestre, P. Andrés, J. J. Miret, and M. V. Andrés, *Opt. Express* **9**, 687 (2001).
8. K. Saitoh, M. Koshiba, T. Hasegawa, and E. Sadaoka, *Opt. Express* **11**, 843 (2003).
9. G. Renversez, B. Kuhlmeier, and R. McPhedran, *Opt. Lett.* **28**, 989 (2003).
10. J. K. Ranka, R. S. Windeler, and A. J. Stentz, *Opt. Lett.* **25**, 25 (2000).
11. W. J. Wadsworth, J. C. Knight, A. Ortigosa-Blanch, J. Arriaga, E. Silvestre, and P. St. J. Russell, *Electron. Lett.* **36**, 53 (2000).
12. Y. F. Li, B. W. Liu, Z. H. Wang, M. L. Hu, Z. Wang, and Q. Y. Wang, *Chin. J. Lasers (in Chinese)* (to be published).
13. K. Kawano and T. Kitoh, *Introduction to Optical Waveguide Analysis: Solving Maxwell's Equations and the Schrödinger Equation* (John Wiley & Sons, New York, 2001) chap. 4.
14. V. Finazzi, T. M. Monro, and D. J. Richardson, *IEEE Photon. Technol. Lett.* **15**, 1246 (2003).
15. W. H. Reeves, J. C. Knight, P. St. J. Russell, and P. J. Roberts, *Opt. Express* **10**, 609 (2002).